Dalton Transactions

PAPER

View Article Online
View Journal

Cite this: DOI: 10.1039/c6dt00567e

Dinickel complexes with anthyridine-based ligands†

Da-Wei Huang, Yi-Hung Liu, Shie-Ming Peng and Shiuh-Tzung Liu*

Received 10th February 2016,
Accepted 5th April 2016

DOI: 10.1039/c6dt00567e

www.rsc.org/dalton

Two new dinickel complexes with anthyridine-based ligands, 5-phenyl-2,8-bis(2-pyridinyl)-1,9,10-anthyridine (**L_2**) and 5-phenyl-2,8-bis(6′-bipyridinyl)-1,9,10-anthyridine (**L_3**), are reported. Complexation of $Ni(OAc)_2$ with **L_2** and **L_3** in trifluoroacetic acid provided the corresponding dinickel complexes $[\{Ni_2(\mathbf{L_2})(H_2O)_6(CF_3COO)_2\}(CF_3COO)_2]$ (**2**) and $[Ni_2(\mathbf{L_3})(CF_3COO)_4(H_2O)]$ (**3**), respectively. Both complexes were characterized by spectroscopic methods and further confirmed by X-ray crystallography. Structural analyses of **2** and **3** revealed the Ni···Ni distances in the complexes to be 5.4086(6) and 5.0138(7) Å, respectively. The catalytic activities of complexes **2** and **3** toward the reduction of carboxylic acids were evaluated. It appears that complex **3** shows a good catalytic activity toward the reduction of carboxylates into the corresponding alcohols by diphenylsilane.

Introduction

The use of bimetallic complexes as catalysts in homogeneous catalysis has received much attention in recent years. A number of investigations have shown that the bimetallic catalyst is significantly more active than the related monometallic ones. It is believed that the "cooperative" interaction of the two metal ions might play a key role in increasing the activity.[1] Among various dinuclear systems, chemists are interested in dinickel complexes, especially as model compounds for dinuclear metallo-enzymes,[2] as catalysts for cross coupling and oxidation,[3,4] as pre-catalysts for olefin polymerization,[5] and to understand and control the reactivity of dinuclear metal species.[6]

In our earlier investigations, the distance between Ni···Ni (3.240 Å) in dinickel complexes $[(\mathbf{L_1})(\mu\text{-}Cl)_2Ni_2Cl_2(CH_3OH)_2]$ (**1**) is shorter than that in urease, showing no catalytic activity toward hydrolysis of urea or amides. However, complex **1** appears to be an excellent catalyst for the homo-coupling of terminal alkynes with the use of O_2 as the oxidant.[4b] In an effort to better understand the inter-metal distances attributed to the cooperative effect, we report the preparation and characterization of dinickel complexes containing anthyridine-based ligands **L_2** and **L_3** (Scheme 1), in which the metal ions are separated by *ca.* 5 Å.[7] The resulting complexes were characterized by both spectroscopic and X-ray crystallographic methods. The catalytic activities of these complexes toward the reduction of carboxylic acids were investigated.

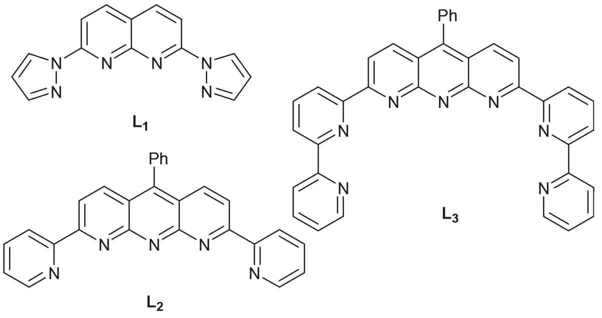

Scheme 1

Results and discussion

Preparation and characterization of dinickel complexes

The multiple dentates **L_2** and **L_3** were prepared according to our earlier work.[7] Heating up a mixture of $Ni(OAc)_2$ and **L_2** in a mixed solvent of methanol and CF_3COOH gave $[\{Ni_2(\mathbf{L_2})(H_2O)_6(CF_3COO)_2\}(CF_3COO)_2]$ (**2**) in 91% yield based on the ligand (eqn (1)), whereas a reaction of **L_3** with $Ni(OAc)_2$ under similar conditions yielded a neutral complex $[Ni_2(\mathbf{L_3})$-

---

Department of Chemistry, National Taiwan University, Taipei 106, Taiwan.
E-mail: stliu@ntu.edu.tw

† Electronic supplementary information (ESI) available: Spectra of complexes 2 and 3; X-ray crystallographic data, structure refinement details, and CIF files for compounds 2 and 3. CCDC 1450223 and 1450222. For ESI and crystallographic data in CIF or other electronic format see DOI: 10.1039/c6dt00567e

(μ-CF_3COO)(CF_3COO)$_3$(H_2O)] (**3**) in 88% yield (eqn (2)). These complexes were characterized by both X-ray structural determination and spectroscopic methods.

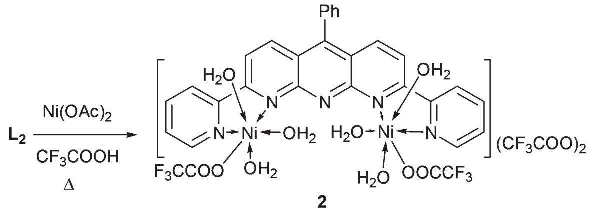

(1)

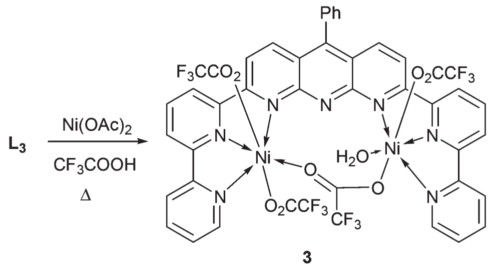

(2)

Light yellow crystals of **2** were grown by vaporization of a mixed solvent system of acetone and methanol at room temperature. The ORTEP plot of the cationic part of **2** is shown in Fig. 1 and selected bond distances and bond angles are collected in Table 1. The two nickel(II) centers are embedded in a distorted octahedral environment in which the coordination geometry of each metal is completed by the "bipyridine" moiety, three water molecules and a trifluoroacetate with all water molecules *cis* to each other. Two nickel centers are separated by 5.4086(6) Å. The central nitrogen donor N(3) of anthyridine remains as a free donor site, but this donor shows hydrogen-bonding interactions with the coordinating water molecules. The distances of N(3)–O(4) and N(3)–O(9) are 3.096(4) and 3.058(4) Å, respectively, within the hydrogen bonding interaction range. The bite angles of N(1)–Ni(1)–N(2) and N(4)–Ni(2)–N(5) are 77.7(1)° and 78.5(1)°, respectively, which are typical of the bipyridine complexes. It is noticed that two nickel ions are not seated in the plane defined by the ligand presumably due to the steric congestion. No significant discrepancies in other bond lengths and angles were noticed in complex **2**.

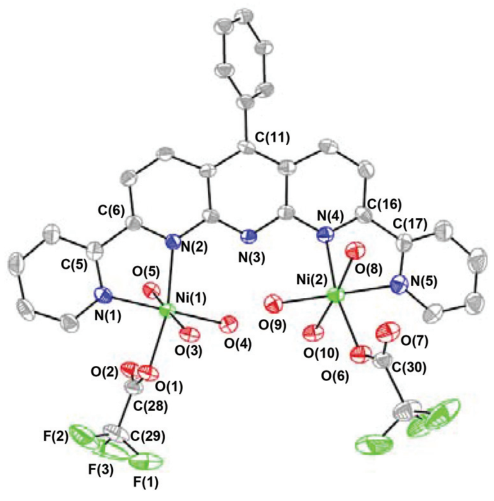

Fig. 1 ORTEP plot of the cationic portion of **2** at the 30% probability level. Labels of aromatic carbons are omitted for clarity.

Table 1 Selected bond distances (Å) and bond angles (°) for **2**

Ni(1)–N(1)	2.063(3)	Ni(2)–N(4)	2.129(3)
Ni(1)–N(2)	2.137(3)	Ni(2)–N(5)	2.058(3)
Ni(1)–O(1)	2.050(3)	Ni(2)–O(6)	2.056(3)
Ni(1)–O(3)	2.037(3)	Ni(2)–O(8)	2.089(3)
Ni(1)–O(4)	2.043(3)	Ni(2)–O(9)	2.020(3)
Ni(1)–O(5)	2.092(3)	Ni(2)–O(10)	2.054(3)
N(1)–Ni(1)–N(2)	77.73(12)	N(4)–Ni(2)–N(5)	78.49(13)
N(2)–Ni(1)–O(1)	167.56(12)	N(4)–Ni(2)–O(6)	168.18(12)
N(1)–Ni(1)–O(4)	176.92(13)	N(5)–Ni(2)–O(9)	177.00(12)
O(3)–Ni(1)–O(5)	174.80(13)	O(8)–Ni(2)–O(10)	175.51(13)
N(1)–Ni(1)–O(5)	88.25(12)	N(4)–Ni(2)–O(10)	91.87(12)
N(2)–Ni(1)–O(5)	86.29(12)	N(5)–Ni(2)–O(10)	94.30(13)

Complex **3** was obtained as a light green crystalline solid. The molecular structure of complex **3** is shown in Fig. 2 and the important structural parameters are summarized in Table 2. The complex has a dinuclear core bridged by a tri-

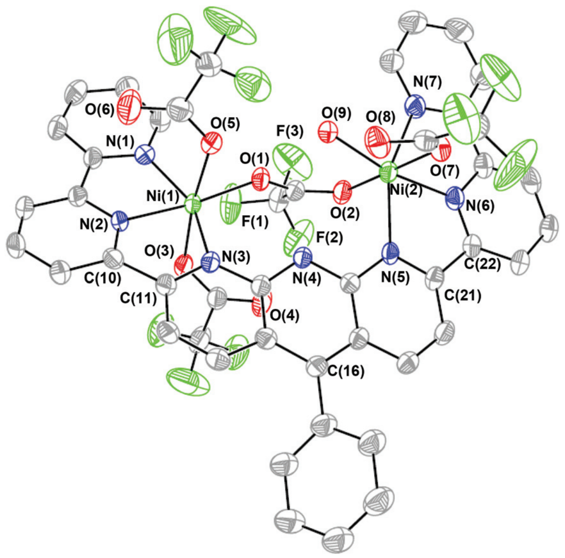

Fig. 2 ORTEP plot of the cationic portion of **3** (30% probability level).

Table 2 Selected bond distances (Å) and bond angles (°) for **3**

Ni(1)–N(1)	2.097(3)	Ni(2)–N(5)	2.139(3)
Ni(1)–N(2)	2.005(3)	Ni(2)–N(6)	2.002(3)
Ni(1)–N(3)	2.157(3)	Ni(2)–N(7)	2.114(3)
Ni(1)–O(1)	2.091(3)	Ni(2)–O(2)	2.072(3)
Ni(1)–O(3)	2.084(3)	Ni(2)–O(7)	2.120(3)
Ni(1)–O(5)	2.047(3)	Ni(2)–O(9)	2.024(3)
N(1)–Ni(1)–N(2)	78.08(12)	N(5)–Ni(2)–N(6)	77.10(13)
N(1)–Ni(1)–N(3)	154.70(12)	N(5)–Ni(2)–N(7)	154.92(13)
N(2)–Ni(1)–O(1)	172.00(12)	N(6)–Ni(2)–O(2)	95.73(13)
N(2)–Ni(1)–O(3)	87.72(12)	N(6)–Ni(2)–O(9)	168.61(13)
O(3)–Ni(1)–O(5)	173.22(10)	O(2)–Ni(2)–O(7)	178.85(11)

fluoroacetate group in the μ^2-1,3-bridging mode, providing a [$Ni_2(\mathbf{L_3})(\mu\text{-}CF_3COO)(CF_3COO)_3(H_2O)$] core with a Ni(1)⋯Ni(2) separation of 5.0138(7) Å. The coordination about the Ni(II) atoms is described as a distorted octahedral geometry. The coordinating ligands around the two nickel centers are slightly different. The Ni(1) center is completed by three nitrogen donors [N(1), N(2) and N(3)] of the "terpyridine" moiety, two oxygen atoms [O(3) and O(5)] from terminal trifluoroacetates and one oxygen atom O(1) of the bridging trifluoroacetate, with two terminal trifluoroacetates occupying apical positions, while the coordination environment of the Ni(2) center is different from that of Ni(1). Besides the tridentate of "terpyridine", a terminal trifluoroacetate, the bridging trifluoroacetate and a water molecule are surrounded at N(2) by two trifluoroacetate oxygen donors [O(2) and O(7)] *trans* to each other. It is noticed that the coordination modes of the bridging trifluoroacetate toward Ni(1) and Ni(2) are different: O(1) is seated at the equatorial plane constituted by the ligand in a *mer*-configuration with Ni(1), whereas O(2) is seated at an apical position around Ni(2). The average Ni–N distances around Ni(1) and Ni(2) are 2.086 and 2.085 Å, respectively (Table 2), which compare well with those observed in the related Ni(II) terpyridine complexes.[8] The bond lengths of Ni–O are in the range of 2.024(3)–2.120(3) Å, as expected. The chelation angles of N(1)–Ni(1)–N(2), N(2)–Ni(1)–N(3), N(5)–Ni(2)–N(6) and N(6)–Ni(2)–N(7) in the dinickel core are much deviated from 90°, which is observed in the related terpyridine metal complex due to the ligand constraint. Although the N(3) donor of anthyridine remains uncoordinated, it participates in intramolecular hydrogen bonding with the hydroxylic H atoms on O(9). The distance between N(3)⋯O(9) is 3.201(4) Å, within the range for hydrogen-bonding interaction.

Electronic absorption spectra for the complexes and free ligands were recorded in acetonitrile (Table 3). In comparison with the free ligands, the absorption bands of complexes were red-shifted, indicating coordination effects. Complexes **2** and **3** show intense ligand to metal charge transfer (LMCT) bands with λ_{max} at 407 and 413 nm, respectively. Each complex exhibits a weak absorption at *ca.* 650 nm, which is assignable to a d–d transition arising from the octahedral nickel center.[9]

The magnetic properties of both complexes **2** and **3** were investigated and their properties are quite similar. Variable-temperature (4–300 K) magnetic susceptibility data were collected on amorphous solids of **3** and the plots of χ_M and μ_{eff} *versus* temperature of **3** are presented in Fig. 3. The magnetic moment is almost constant (3.89μ_B) at high temperatures and decreases below 25 K, reaching 3.61μ_B at 4 K (for **2**, μ_{eff} = 3.60 at room temperature, 3.07 at 4 K). The experimental magnetic data have been fitted using eqn (3) with the spin Hamiltonian $-JS_1S_2$ ($S_1 = S_2 = 1$).[10] The fitted values are g = 2.14, J = −0.76 cm^{-1} in **3**, and g = 1.97, J = −0.59 cm^{-1} in **2**. Both complexes are paramagnetic with a weakly antiferromagnetic coupling between the adjacent metal ions due to the long separation (>5 Å).

$$\chi = \frac{2Ng^2\beta^2\left(e^{J/kT} + 5e^{3J/kT}\right)}{kT\left(1 + 3e^{J/kT} + 5e^{3J/kT}\right)} \tag{3}$$

Table 3 UV-vis absorption data for ligands L_2–L_3 and complexes **2**–**3**[a]

Compound	λ_{max} in nm (ε)
$\mathbf{L_2}$	248 (2.95×10^4), 289 (3.29×10^4), 377 (1.76×10^4), 394 (2.02×10^4)
$\mathbf{L_3}$	204 (2.35×10^4), 266 (3.36×10^4), 383 (1.92×10^4), 402 (2.33×10^4)
2	252 (1.76×10^4), 292 (1.53×10^4), 407 (1.68×10^4), 653 (1.3×10^2)
3	241 (5.34×10^4), 279 (4.42×10^4), 396 (2.41×10^4), 413 (2.66×10^4), 650 (1.60×10^2)

[a] In acetonitrile.

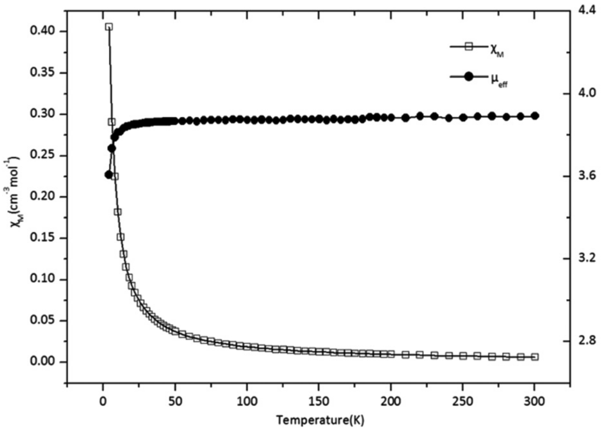

Fig. 3 Plots of χ_M (□) and μ_{eff} (•) *vs.* T for **3**. The solid line corresponds to the theoretical fit.

Catalysis–reduction of carboxylic acids

The reduction of carboxylic acids to yield the corresponding alcohols is a straightforward and useful method to produce the desired precursors in organic synthesis. Among various strategies, the metal-catalyzed hydrosilylation of carboxylate moieties for this reduction ought to be a safe and operationally simple method. However, only a limited number of homogeneously catalytic systems have been applied for the hydrosilylation of carboxylates including ruthenium,[11] boron,[12] indium,[13] iron[14] and main group Lewis acid[15] compounds. There is no documentation on the use of a nickel complex as the catalyst for such a reduction. Thus, the activity of complexes **2** and **3** toward the hydrosilylation of carboxylic acids was investigated. In particular, we hope that dimetallic systems may assist the reduction through a synergic effect. Thus, searching for the optimal conditions for the reduction of benzoic acid leading to benzyl alcohol catalysed by complex **3** was initially examined (Table 4).

A series of screen tests with various reducing agents suggested that carrying out the reaction by using diphenylsilane under refluxing conditions in THF provided the desired product in 31% yield (Table 4, entry 5). By using varying sol-

Table 4 Reduction of PhCOOH under various conditions catalysed by **3**[a]

Entry	Reductant	Solvent	Temp.	Yield[b]
1	H_2 (200 psi)	THF	65 °C	0
2	H_2 (200 psi)/Zn (0.4 mmol)	THF	65 °C	0
3	$NaBH_4$ (0.8 mmol)	THF	65 °C	Trace
4	HCOONa (0.8 mmol)/Zn	THF	65 °C	0
5	Ph_2SiH_2 (0.8 mmol)	THF	65 °C	31%
6	Ph_2MeSiH (0.8 mmol)	THF	65 °C	<10%
7	$PhMe_2SiH$ (0.8 mmol)	THF	65 °C	12%
8	Ph_2SiH_2 (0.8 mmol)	MeOH	65 °C	Trace
9	Ph_2SiH_2 (0.8 mmol)	1,4-Dioxane	100 °C	45%
10	Ph_2SiH_2 (0.8 mmol)	DMF	100 °C	Trace
11	Ph_2SiH_2 (0.8 mmol)	Toluene	110 °C	<10%

[a] Reaction conditions: benzoic acid (0.2 mmol) and complex **3** (1×10^{-2} mmol) in solvent (0.5 mL) for 16 h. [b] Isolated yields.

vents, it was found that the yield of $PhCH_2OH$ increased up to 45% with the use of dioxane as the solvent (Table 4, entry 9). Apparently, these results were not good enough for the synthetic applications. Further modification of the reaction conditions by the addition of bases or auxiliary ligands was investigated. Table 5 summarizes the results. The addition of bases into the reactions did not increase the production of the desired compound (Table 5, entries 3–5). To our delight, carrying out the reduction in the presence of phosphine provided better results (Table 5, entries 6–8). Particularly, the addition of 5 mol% of tributylphosphine did assist the reduction smoothly to render benzoic acid in 82% yield (Table 5, entry 7). It is noticed that the use of bidentate or bulky phosphine ligands provided poor results. Under these optimal conditions, the amount of silane used for the reduction was studied (Table 5, entries 13 and 14). It shows that carrying out the reaction with the use of 4 equimolar amounts of Ph_2SiH_2 is the best choice.

Table 5 Reduction of PhCOOH catalysed by **3** with various additives[a]

Entry	Additives	Yield[b]
1	—	45%
2	n-Bu_4NBr (0.2 mmol)	48%
3	Na_2CO_3 (0.2 mmol)	21%
4	Pyridine (0.2 mmol)	16%
5	DBU (0.2 mmol)	52%
6	PPh_3 (0.02 mmol)	63%
7	$P(n\text{-}Bu)_3$ (0.02 mmol)	82%
8	$P(n\text{-}Bu)_3$ (0.04 mmol)	84%
9	$P(n\text{-}Bu)_3$ (0.01 mmol)	69%
10	PCy_3 (0.02 mmol)	38%
11	Ethylenediamine (0.2 mmol)	23%
12	$Ph_2PCH_2CH_2PPh_2$ (0.02 mmol)	70%
13[c]	$P(n\text{-}Bu)_3$ (0.04 mmol)	61%
14[d]	$P(n\text{-}Bu)_3$ (0.04 mmol)	27%
15[e]	$P(n\text{-}Bu)_3$ (0.04 mmol)	—

[a] Reaction conditions: benzoic acid (0.2 mmol), complex **3** (5 mol%, 1×10^{-2} mmol) and Ph_2SiH_2 (0.8 mmol) in dioxane (0.5 mL) at 100 °C for 16 h. [b] NMR yields. [c] Ph_2SiH_2 (0.6 mmol). [d] Ph_2SiH_2 (0.4 mmol). [e] No complex **3** in the reaction.

In order to demonstrate the unique activity of **3** in the catalysis, the ability of various nickel complexes for this catalytic reduction was evaluated and the observations are summarized in Table 6. Quite obviously, complex **3** proved to have the best activity toward this oxidation. Other nickel complexes were tested as catalyst precursors and exhibited some activity, but not as good as complex **3**, including the dinickel complexes associated with ligand $\mathbf{L_1}$ or **dpnp** (Table 6, entries 8 and 9). To our surprise, the catalytic activity of **2** is not as good as that of **3**, presumably due to the slightly longer separation of Ni⋯Ni ions in **2**.

A comparison of the reaction rates catalyzed by **3**, **2** and other Ni complexes was made and the yields of benzyl alcohol *versus* reaction time are summarized in Fig. 4. It appears that there is an induction period for this catalysis. Based on the pseudo-first order approximation, the values of k_{obs} for the pre-catalyst **3**, **2**, $Ni(CF_3COO)_2$/Terpy, $Ni(CF_3COO)_2$/Bipy and $Ni(CF_3COO)_2$ were estimated to be 4.02×10^{-5}, 8.68×10^{-6}, 7.77×10^{-6}, 5.58×10^{-6} and 1.43×10^{-6} (s^{-1}), respectively. The catalytic activity of complex **3** is about 5 times faster than that of complex **2**, and is much better than those of other Ni(II) complexes. Both complexes **2** and **3** are well defined bimetallic

Table 6 Catalytic activity of various nickel complexes[a]

Entry	Nickel complex	Yield[b]
1	**3** (0.01 mmol, 5 mol%)	82%
2	**2** (0.01 mmol, 5 mol%)	43%
3	$Ni(CF_3COO)_2$ (0.02 mmol, 10 mol%)	Trace
4	Terpy/$Ni(CF_3COO)_2$ (0.02/0.02 mmol, 10 mol%)	27%
5	Bipy/$Ni(CF_3COO)_2$ (0.02/0.02 mmol, 10 mol%)	19%
6	$NiCl_2$ (0.02 mmol, 10 mol%)	Trace
7	$Ni(OAc)_2$ (0.02 mmol, 10 mol%)	14%
8	**dpnp**[c]/$Ni(CF_3COO)_2$ (0.01/0.02 mmol, 10 mol%)	29%
9	$\mathbf{L_1}$/$Ni(CF_3COO)_2$ (0.01/0.02 mmol, 10 mol%)	40%

[a] Reaction conditions: benzoic acid (0.2 mmol), Ph_2SiH_2 (0.8 mmol), $P(n\text{-}Bu)_3$ (0.02 mmol) and Ni(II) complex in dioxane (0.5 mL) at 100 °C for 16 h. [b] NMR yields based on the internal standard of mesitylene. [c] **dpnp** = 2,7-dipyridinyl-1,8-naphthyridine.

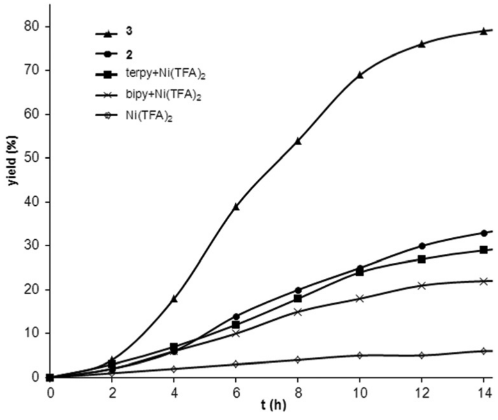

Fig. 4 Product yields along the reaction time catalysed by nickel complexes.

Table 7 Reduction carboxylate derivatives catalyzed by **3**[a]

Entry	Substrate	Product	Yield[b]
1	C_6H_5COOH	$C_6H_5CH_2OH$	82%
2	C_6F_5COOH	$C_6F_5CH_2OH$	35%
3	*p*-MeC_6H_4COOH	*p*-$MeC_6H_4CH_2OH$	85%
4	*p*-ClC_6H_4COOH	*p*-$ClC_6H_4CH_2OH$	77%
5	*p*-$(CN)C_6H_4COOH$	*p*-$(CN)C_6H_4CH_2OH$	72%
6	*p*-$(MeO_2C)C_6H_4COOH$	*p*-$(MeO_2C)C_6H_4CH_2OH$	43%
7	C_6H_5COOMe	$C_6H_5CH_2OH$	36%
8	*p*-$(OHC)C_6H_4COOH$	*p*-$(HOCH_2)C_6H_4CH_2OH$	75%
9	C_6H_5CHO	$C_6H_5CH_2OH$	89%
10	*o*-$C_6H_4(COOH)_2$	—	—
11	2-Pyridinecarboxylic acid	—	—
12	$C_6H_5CH{=}CHCOOH$	$C_6H_5CH{=}CHCH_2OH$	80%
13	$C_6H_5CH_2COOH$	$C_6H_5CH_2CH_2OH$	77%
14	$CH_3(CH_2)_6COOH$	$CH_3(CH_2)_6CH_2OH$	74%
15	$CH_3(CH_2)_4COOH$	$CH_3(CH_2)_4CH_2OH$	66%
16	$C_6H_5CONH_2$	—	—

[a] Reaction conditions: substrate (0.2 mmol), Ph_2SiH_2 (0.8 mmol), P(*n*-Bu)$_3$ (0.02 mmol) and complex **3** (5 mol%, 1×10^{-2} mmol) in dioxane (0.5 mL) at 100 °C for 16 h. [b] Isolated yields.

systems, but the catalytic activity of **3** is superior to that of **2**, indicating the important role of ligand $\mathbf{L_3}$ in the reaction.

We next explored the reduction of various carboxylic acids under the optimal conditions (Table 7). Both substituted benzoic acids and aliphatic carboxylic acids smoothly participated in the reduction to afford the corresponding alcohols in moderate to good yields except for some functionality present in the molecule. Reduction of benzoic acids was amenable with functional groups such as alkyl (entry 3), halo (entry 4) and cyano (entry 5) delivering the corresponding benzyl alcohols in 62%–85% yields. However, both ester and aldehyde functionalities were reduced simultaneously (entries 6–8). It is noticed that the reduction rate of an ester is slower than that of a carboxylic acid. Thus, we were able to obtain 43% isolated yield for the reduction of *p*-$(MeO_2C)C_6H_4COOH$. Reduction of cinnamic acid and aliphatic carboxylic acids gave cinnamyl alcohol and alkanols in good yields (entries 12–15). However, the amide functionality remains intact under the catalytic conditions.

Summary

We have prepared two new dinickel complexes **2** and **3** with anthyridine-based ligands $\mathbf{L_2}$ and $\mathbf{L_3}$. The distances between two nickel centers in complexes **2** and **3** are *ca*. 5.4086(6) and 5.0138(7) Å, respectively. From the experimental data, we believe that both the chelation effect of the terpyridine moiety and the short distance between nickel ions might play a key role for the good catalytic activity of **3** as compared to **2**. We are delighted to learn that the dinickel complex **3** is an effective catalyst for the reduction of various carboxylic acids to give the corresponding alcohols. Further studies of the catalytic activities of both complexes in other reactions are currently in progress.

Experimental

General information

All the reactions, manipulations and purification steps were performed under a dry nitrogen atmosphere. Chemicals and solvents were of analytical grade and were used after a degassing process. Ligands $\mathbf{L_2}$ and $\mathbf{L_3}$ were prepared according to the method reported previously.[7] Nuclear magnetic resonance spectra were recorded in $CDCl_3$ on a Bruker AVANCE 400 spectrometer. Chemical shifts are given in parts per million relative to Me_4Si for ^1H and ^{13}C NMR. Molar magnetic susceptibility was recorded using a SQUID system with a 2000 G external magnetic field.

Preparation of complex 2

A mixture of $\mathbf{L_2}$ (50 mg, 0.12 mmol) and $Ni(OAc)_2{\cdot}4H_2O$ (64.7 mg, 0.26 mmol) in a round bottom flask was flashed with nitrogen for 10 min. A mixture of methanol and CF_3COOH (1 : 1, 3 mL) was added. The mixture was heated to reflux under nitrogen for 24 h. After the reaction, solvents were removed under reduced pressure. The residue was dissolved in methanol and the solution was filtered through Celite. Ether was slowly added to the filtrate and the desired complex was crystallized from the solution as a light-yellow crystalline solid (120 mg, 91%). ESI-HRMS *m*/*z* calcd for $C_{33}H_{17}F_9N_5Ni_2O_6$ $[M - (CF_3COO) - (H_2O)_6]$: 865.9742; found: 865.9744. IR (KBr) ν = 1679 (C=O), 1445, 1137 cm^{-1}. Anal. Calcd for $C_{35}H_{29}F_{12}N_5Ni_2O_{14}$: C, 38.60; H, 2.68; N, 6.43. Found: C, 38.74; H, 2.81; N, 6.25.

Preparation of complex 3

The procedure is quite similar to that used for the preparation of **2**, except for the quantity: $\mathbf{L_3}$ (50 mg, 0.09 mmol) and $Ni(OAc)_2{\cdot}4H_2O$ (47.3 mg, 0.19 mmol). The desired complex was obtained as a green crystalline solid (93.7 mg, 88%): ESI-HRMS *m*/*z* calcd for $C_{41}H_{32}F_6N_7Ni_2O_9$ $[M - (CF_3COO)_2 + (OH) + (H_2O)_3]$: 990.0873; found: 990.0820. IR (KBr) ν = 1676 (C=O), 1451, 1140 cm^{-1}. Anal. Calcd for $C_{45}H_{25}F_{12}N_7Ni_2O_9$: C, 46.87; H, 2.19; N, 8.50. Found: C, 46.68; H, 2.31; N, 8.42.

Crystallography

Crystals suitable for X-ray determination were obtained for $\mathbf{2}{\cdot}(CH_3COCH_3)_2(H_2O)_2$ and $\mathbf{3}{\cdot}(CH_3COCH_3)(CH_3CH_2OCH_2CH_3)$ by recrystallization. Cell parameters were determined using a Siemens SMART CCD diffractometer. The structure was solved using the SHELXS-97 program[16] and refined using the SHELXL-97 program[17] by full-matrix least-squares on F^2 values. Crystal data of these complexes are listed in the ESI.† Other crystallographic data are deposited in the ESI.†

Crystal data for **2**: yellow colour, column, $C_{41}H_{44}F_{12}N_5Ni_2O_{18}$, F_w = 1240.23, monoclinic, $P2(1)/c$, a = 16.6454(7) Å, b = 14.6305(8) Å, c = 21.2591(10) Å, α = 90, β = 90.049(4)°, γ = 90, V = 5177.2(4) Å^3, Z = 4, D_{calcd} = 1.591 Mg m^{-3}, $F(000)$ = 2532, crystal size: 0.20 × 0.15 × 0.10 mm^3, 2.82 to 25.00°, 25 095 reflections collected, 8809 reflections [R(int) = 0.0444], final R indices [$I > 2\text{sigma}(I)$]: R_1 = 0.0401, wR_2 = 0.0893, for all data R_1 = 0.0540, wR_2 = 0.0975, goodness-of-fit on F^2 = 1.039.

Crystal data for **3**: yellow colour, plate, $C_{52}H_{39}F_{12}N_7Ni_2O_{11}$, F_w = 1283.32, monoclinic, $P2(1)/c$, a = 20.1055(6) Å, b = 18.0229(5) Å, c = 15.0825(5) Å, α = 90°, β = 90.727(3)°, γ = 90°, V = 5464.8(3) Å^3, Z = 4, D_{calcd} = 1.560 Mg m^{-3}, F(000) = 2608, crystal size: 0.25 × 0.15 × 0.10 mm^3, 2.82 to 25.00°, 27 720 reflections collected, 9191 reflections [R(int) = 0.0476]. The disordered solvent in the crystal was refined by the use of SQUEEZE. The total potential volume for solvent molecules is 229.0 Å^3 in the per unit cell volume 5464.9 Å^3 [4.2%]. Final R indices [I > 2sigma(I)]: R_1 = 0.0536, wR_2 = 0.1324, for all data R_1 = 0.0828, wR_2 = 0.1506, goodness-of-fit on F^2 = 1.032.

Catalysis–reduction of carboxylic acids

A reaction tube loaded with a mixture of carboxylic acid (0.2 mmol), diphenylsilane (0.8 mmol), Ni complex **3** (1×10^{-2} mmol), and P(n-Bu)$_3$ (0.02 mmol) in dioxane (0.5 mL) was heated at 100 °C for 16 h. After the reaction, brine (2 mL) was added to the reaction mixture and then extracted with ether (3 mL × 3). The combined organic extracts were dried and concentrated. The residue was analysed by NMR spectroscopy. For the purification, chromatography on silica gels provided the desired compound in the pure form. The spectral data of the organic products are essentially identical to the reported ones.

Benzyl alcohol. ^{1}H NMR (400 MHz, CDCl$_3$): δ 7.48–7.32 (m, 5H), 4.63 (s, 2H), 2.51 (s, 1H). ^{13}C NMR (100 MHz): δ 141.1, 128.2, 127.9, 127.3, 64.9.

***p*-Methylbenzyl alcohol.** ^{1}H NMR (400 MHz, CDCl$_3$): δ 7.30 (m, 2H), 7.17 (m, 2H), 4.68 (s, 2H), 2.42 (s, 3H), 1.81 (s, 1H). ^{13}C NMR (100 MHz): δ 138.2, 137.1, 128.9, 127.4, 65.0, 20.9.

***p*-Chlorobenzyl alcohol.** ^{1}H NMR (400 MHz, CDCl$_3$): δ 7.39–7.25 (m, 4H), 4.61 (s, 2H), 2.18 (s, 1H). ^{13}C NMR (100 MHz): δ 139.0, 133.6, 129.1, 128.4, 64.1.

***p*-Cyanobenzyl alcohol.** ^{1}H NMR (400 MHz, CDCl$_3$): δ 7.61 (m, 2H), 7.50 (m, 2H), 4.72 (s, 2H), 2.73 (s, 1H). ^{13}C NMR (100 MHz): δ 146.2, 132.6, 127.2, 119.1, 111.2, 64.3.

***p*-(Methoxycarbonyl)benzyl alcohol.** ^{1}H NMR (400 MHz, CDCl$_3$): δ 8.03 (d, J = 8.2 Hz, 2H), 7.45 (d, J = 8.2 Hz, 2H), 4.74 (s, 2H), 3.88 (s, 3H), 2.35 (bs, 1H). ^{13}C NMR (100 MHz): δ 166.8, 146.3, 129.4, 129.1, 126.3, 64.6, 51.9.

***p*-(Methoxymethyl)benzyl alcohol.** ^{1}H NMR (400 MHz, CDCl$_3$): δ 7.41 (s, 4H), 4.73 (s, 4H). ^{13}C NMR (100 MHz): δ 140.6, 127.4, 65.5.

3-Phenylprop-2-en-1-ol. ^{1}H NMR (400 MHz, CDCl$_3$): δ 7.43 (m, 2H), 7.34 (m, 2H), 7.28 (m, 1H), 6.61 (d, J = 14.7 Hz, 1H), 6.41 (m, 1H), 4.34 (m, 2H). ^{13}C NMR (100 MHz, CDCl$_3$): δ 136.9, 131.0, 128.7, 128.5, 127.9, 126.2, 64.0.

2-Phenylethanol. ^{1}H NMR (400 MHz, CDCl$_3$): δ 7.41–7.34 (m, 2H), 7.32–7.23 (m, 3H), 3.92–3.83 (m, 2H), 2.89 (t, J = 7.4 Hz, 2H), 2.02 (s, 1H). ^{13}C NMR (100 MHz): δ 138.8, 129.2, 128.3, 126.6, 63.8, 39.1.

1-Octanol. ^{1}H NMR (400 MHz, CDCl$_3$): δ 3.63 (t, J = 7.5 Hz, 2H), 1.57 (m, 2H), 1.28 (m, 10H), 0.84 (t, J = 7.1 Hz, 3H). ^{13}C NMR (100 MHz): δ 62.9, 33.1, 32.3, 29.6, 29.2, 25.6, 22.1, 14.4.

1-Hexanol. ^{1}H NMR (400 MHz, CDCl$_3$): δ 3.65 (t, J = 7.2 Hz, 2H), 1.55 (m, 2H), 1.33 (m, 6H), 0.87 (t, J = 7.4 Hz, 3H). ^{13}C NMR (100 MHz): δ 63.8, 32.9, 31.8, 25.3, 22.7, 14.1.

Acknowledgements

We thank the Ministry of Science and Technology, Taiwan for financial support (MOST103-2113-M-002-MY3).

References

1 (*a*) M. Boiocchi and L. Fabbrizzi, *Chem. Soc. Rev.*, 2014, **43**, 1835; (*b*) J.-P. Launay, *Coord. Chem. Rev.*, 2013, **257**, 1544; (*c*) Y. Sunatsuki, R. Kawamoto, K. Fujita, H. Maruyama, T. Suzuki, H. Ishida, M. Kojima, S. Iijima and N. Matsumoto, *Coord. Chem. Rev.*, 2010, **254**, 1871; (*d*) K. P. Kornecki, J. F. Berry, D. C. Powers and T. Ritter, *Prog. Inorg. Chem.*, 2014, **58**, 225; (*e*) L. Noodleman, W.-G. Han Du, J. A. Fee, A. W. Gotz and R. C. Walker, *Inorg. Chem.*, 2014, **53**, 6458; (*f*) K. Mashima, Y. Hayashi, K. Agura and T. Ohshima, *Pure Appl. Chem.*, 2014, **86**, 335; (*g*) P. Haack and C. Limberg, *Angew. Chem., Int. Ed.*, 2014, **53**, 4282, and references therein.

2 (*a*) C. He and S. J. Lippard, *J. Am. Chem. Soc.*, 2000, **122**, 184; (*b*) F. Meyer, *Prog. Inorg. Chem.*, 2009, **56**, 487; (*c*) W.-Z. Lee, H.-S. Tseng, T.-L. Wang, H.-L. Tsai and T.-S. Kuo, *Organometallics*, 2010, **29**, 2874, and references therein.

3 (*a*) S. Pal and C. Uyeda, *J. Am. Chem. Soc.*, 2015, **137**, 8042; (*b*) T. J. Steiman and C. Uyeda, *J. Am. Chem. Soc.*, 2015, **137**, 6104; (*c*) A. Velian, S. Lin, A. J. M. Miller, M. W. Day and T. Agapie, *J. Am. Chem. Soc.*, 2010, **132**, 6296; (*d*) N. P. Mankad, *Synlett*, 2014, 1197.

4 (*a*) J. Wallick, C. G. Riordan and G. P. A. Yap, *J. Am. Chem. Soc.*, 2013, **135**, 14972; (*b*) T.-P. Cheng, B.-S. Liao, Y.-H. Liu, S.-M. Peng and S.-T. Liu, *Dalton Trans.*, 2012, **41**, 3468; (*c*) J. Lach, A. Jeremies, V. Lozan, C. Loose, T. Hahn, J. Kortus and B. Kersting, *Inorg. Chem.*, 2012, **51**, 12380; (*d*) A. Bheemaraju, J. W. Beattie, E. G. Tabasan, P. D. Martin, R. L. Lord and S. Groysman, *Organometallics*, 2013, **32**, 2952; (*e*) J. Ferrando-Soria, O. Fabelo, M. Castellano, J. Cano, S. Fordham and H.-C. Zhou, *Chem. Commun.*, 2015, **51**, 13381.

5 (*a*) Q. Xing, K. Song, T. Liang, Q. Liu, W.-H. Sun and C. Redshaw, *Dalton Trans.*, 2014, **43**, 7830; (*b*) J. P. McInnis, M. Delferro and T. J. Marks, *Acc. Chem. Res.*, 2014, **47**, 2545. (Polymerization).

6 (*a*) A. Jeremies, U. Lehmann, S. Gruschinski, F. Schleife, M. Meyer, V. Matulis, O. A. Ivashkevich, M. Handke, K. Stein and B. Kersting, *Inorg. Chem.*, 2015, **54**, 3937; (*b*) G. L. Guillet, J. B. Gordon, G. N. Di Francesco, M. W. Calkins, E. Cizmar, K. A. Abboud, M. W. Meisel, R. Garcia-Serres and L. J. Murray, *Inorg. Chem.*, 2015, **54**, 2691; (*c*) W. J. Schreiter, A. R. Monteil, E. Kalachnikova, M. A. Peterson, M. D. Moulis, C. D. Gasery,

G. T. McCandless, F. R. Fronczek and G. G. Stanley, *Inorg. Chem.*, 2015, **54**, 10036; (*d*) J. P. S. Walsh, S. Sproules, N. F. Chilton, A.-L. Barra, G. A. Timco, D. Collison, E. J. L. McInnes and R. E. P. Winpenny, *Inorg. Chem.*, 2014, **53**, 8464; (*e*) R. Beck and S. A. Johnson, *Organometallics*, 2013, **32**, 2944, and references therein.

7 D.-w. Huang, Y.-H. Liu, S.-M. Peng and S.-T. Liu, *Organometallics*, 2016, **35**, 151.

8 M. G. Barandika, R. Cortés, L. Lezama, M. K. Urtiaga, M. I. Arriortuac and T. Rojo, *J. Chem. Soc., Dalton Trans.*, 1999, 2971–2976.

9 (*a*) S. Datta, D. K. Seth, R. J. Butcher and S. Bhattacharya, *Inorg. Chim. Acta*, 2011, **377**, 120; (*b*) U. Lehmann, J. Klingele, V. Lozan, G. Steinfeld, M. H. Klingele, S. Käss, A. Rodenstein and B. Kersting, *Inorg. Chem.*, 2010, **49**, 11018.

10 F.-M. Nie, J. Chen and F. Lu, *Inorg. Chim. Acta*, 2011, **365**, 190.

11 (*a*) J. A. Fernández-Salas, S. Manzini and S. P. Nolana, *Adv. Synth. Catal.*, 2014, **356**, 308; (*b*) K. Miyamoto, Y. Motoyama and H. Nagashima, *Chem. Lett.*, 2012, **41**, 229.

12 (*a*) D. Bézier, S. Park and M. Brookhart, *Org. Lett.*, 2013, **15**, 496; (*b*) V. Gevorgyan, M. Rubin, J.-X. Liu and Y. Yamamoto, *J. Org. Chem.*, 2001, **66**, 1672.

13 N. Sakai, K. Kawana, R. Ikeda, Y. Nakaike and T. Konakahara, *Eur. J. Org. Chem.*, 2011, 3178.

14 L. C. Misal Castro, H. Li, J.-B. Sortais and C. Darcel, *Chem. Commun.*, 2012, **48**, 10514.

15 (*a*) D. W. Stephan, *Acc. Chem. Res.*, 2015, **48**, 306; (*b*) D. J. Parks, J. M. Blackwell and W. E. Piers, *J. Org. Chem.*, 2000, **65**, 3090.

16 G. M. Sheldrick, SHELXS-90, *Acta Crystallogr., Sect. A: Found. Crystallogr.*, 1990, **46**, 467.

17 G. M. Sheldrick, SHELXL-97, University of Göttingen, Göttingen, Germany, 1997.